Growth of magnetic tunnel junctions on Si(001) substrates

S. Olive Mendez, V. Le Thanh, I. Ozerov, S. Ferrero. C. Coudreau, J.L. Lazzari, F. Arnaud d' Avitaya, L. Ravel, P. Boivin.

Abstract

We present in this work the growth of magnetic tunnel junctions on Si(001) substrates using a template layer technique and the implementation of the layer-by-layer method to form the oxide barrier layer. By using a Co_2Si template layer formed by deposition of Co on Si at a temperature of ~300 °C, we show that it is possible to considerably reduce the reaction between transition metals with Si substrate. We have also investigated the growth of alumina (Al_2O_3) barrier layer by an alternative layer-by-layer deposition method, which consists of successive cycles of molecularbeam deposition of an Al monolayer and oxidation under an O_2 flux at room temperature. Numerous Co(Fe)/AlO_x/NiFe tunnel junctions have been fabricated on Si(001) substrates. The oxidation kinetics, the surface morphology as well as the interface roughness and abruptness are studied by means of Auger profilometry, transmission electron microscopy and atomic force microscopy. We show that it is possible to realize a uniform and homogeneous nanometer-thick AlO_x layer with smooth and sharp interfaces. Current–voltage and Kerr effect measurements are also used to investigate the electric and magnetic properties of these junctions.

Keywords: Layer-by-layer deposition; Nanometer-scaled oxide barrier; Magnetic tunnel junctions; Magnetic Random Access Memories (MRAM)

Introduction

In recent years, much work has been devoted to the fabrication of magnetic tunnel junctions (MTJ) both for their interest in physics and their potential applications in Magnetic Random Access Memories (MRAM) [1–3]. A magnetic tunnel junction basically consists of two ferromagnetic metallic electrodes separated by a nanometer-scaled oxide barrier layer. Such a layering structure can display a large change in resistance when the magnetization directions of two ferromagnetic layers change from parallel to antiparallel orientations. This effect has been explained by the spin-dependent electron tunneling across the barrier layer and reflects the spin asymmetry in the electron density of states of the magnetic layers at the interfaces [4].

The integration of the MRAM fabrication process in the silicon technology represents a crucial issue for their future development. Actually, for MRAM fabrication, the magnetic tunnel junctions are deposited onto a properly planarized complementary metal–oxide–semiconductor (CMOS) wafer in which transistors, diodes and word lines have been already incorporated. After the deposition stage, the metallization process can take place in order to connect the junctions in the memory matrix. This technology implies that the whole components of the junction, the ferromagnetic electrodes and the thin oxide layer, should be deposited on SiO_2 or Cu/SiO_2, on which the control of both surface roughness and film thickness uniformity still remains a challenge.

It is worth noting that in MRAM structures, epitaxial MgO is usually used as a tunnel barrier and the achieved value of tunneling magnetoresistance (TMR) can be as high as 350% [5,6]. The formation of the epitaxial MgO barrier requires correct crystalline orientation of the ferromagnetic electrodes to achieve lattice matching at the interfaces between the electrodes and the tunnel barrier. Since MgO has a bcc

structure, it is desirable to use bcc-structured electrodes (bcc Co, bcc Fe or an alloy of two). Because it is difficult to grow bcc Co or bcc Fe with texture oriented along (001) direction, the development of structures like (CoFe)B/MgO/(CoFe)B has provided a practical solution to overcome this difficulty [7].

We report in this paper the growth of magnetic tunnel junctions with amorphous (Al_2O_3) barrier layers. The advantage for the use of Al_2O_3 as barrier layer is that Al_2O_3 is a very dense oxide and the oxygen bonding energy in Al_2O_3 is relatively high (>3 eV). In previous works, the Al_2O_3 barrier layer was formed by natural and plasma oxidation [8–10]. In our work, we use room temperature oxidation under a molecular O_2 flux. The studied structures are Co(Fe)/AlO_x/NiFe and we show that it is possible to grow these structures on Si(001) substrates by the use of a template technique to prevent the formation of disordered silicides at the interface between a transition metal and Si. We show that when depositing cobalt on Si at a substrate temperature of about 300 °C, an epitaxial Co_2Si silicide can be formed. This phase consists of small domains with c-axis perpendicular to the film surface while the in-plane axes are randomly oriented. Ferromagnetic Co or CoFe layers grown on this Co_2Si template layer at room temperature are shown to have a surface roughness much smaller than that of the layers directly deposited on Si substrates. We have also investigated the formation of the AlO_x tunnel barrier via the layer-bylayer growth method, which consists of successive cycles of molecular-beam deposition of an Al monolayer and oxidation under an O_2 flux. Structural analyses from cross-sectional transmission electron microscopy (TEM) reveal that a relatively flat and uniform nanometer-thick oxide layer can be obtained by using this layer-by-layer approach. While the precise stoichiometry

of the oxide layer remains to be determined, Kerr effect measurements performed on an MTJ stacks with an oxide layer fabricated by this technique suggest that its overall quality is at least similar to the one oxidized in ambient air.

Experimental details

Experiments were carried out in two growth systems. One system is a standard Riber Molecular Beam Epitaxial (MBE) system consisting of a growth chamber and a separate chamber for oxidation. The growth chamber is equipped with reflection highenergy electron diffraction (RHEED), effusion cells for evaporation of Ni, Fe and Al, and an e-gun for Co deposition. In all experiments, theAl growth rate is∼1monolayer (ML)/min while the growth rates for transition metals are about 4–5 ML/min. The oxidation chamber is equipped with an oxygen injector; the oxygen pressure during oxidation process varied from 10^{-9} to 10^{-4} Torr. The substrate temperature during Al oxidation is kept at room temperature. The second growth system is equipped with a scanning tunneling microscopy (STM) and low-energy electron diffraction (LEED) for studying the early stages of the formation of the template layers on Si substrates.

The Si substrates were chemically cleaned following the modified Shiraki method [11]. The thin surface oxide layer was removed by heating the sample at ∼850 °C for 10–15 min. After the oxide desorption, RHEED patterns exhibit a well-developed 2×1 diagrams, no traces of silicon carbide were detected from RHEED. The substrate temperature was measured by a thermocouple in contact with the back site of the substrate.

After growth, the film composition, surface morphology, structures and magnetic properties were measured by means of Auger profilometry, AFM, cross-sectional TEM and magnetooptical Kerr effect (MOKE). AFM images were recorded with a Digital Instruments Nanoscope III setup operating in tapping mode. The film structure and also the interface roughness were investigated by TEM using a JEOL 3010-FX electron microscope working at 300 kV with spatial resolution of 1.7 Å. Magnetic properties of the films have been analyzed by longitudinal MOKE at grazing incidence (about 40°) using s-polarized light of a He–Ne laser at 632.8 nm. The light reflected from the sample surface has been detected behind a Glann prism analyzer by a photodiode. The external magnetic field has been applied in the film plane.

Results and discussion

In order to test layer-by-layer approach for growing the oxide layer in Co(Fe)/AlO_x/NiFe tunnel junctions, it is important to control the surface roughness of the bottom Co(Fe) ferromagnetic electrode. Indeed, since layer-by-layer approach consists of successive cycles of aluminium deposition with monolayer thickness followed by oxidation, it is expected that the bottom electrode, which also serves as a support for growing the oxide layer, should have a surface roughness as small as possible. Furthermore, because the whole thickness of the oxide barrier is in order of ~2 nm, a surface roughness higher than this value should certainly lead to a poor performance of the MTJ.

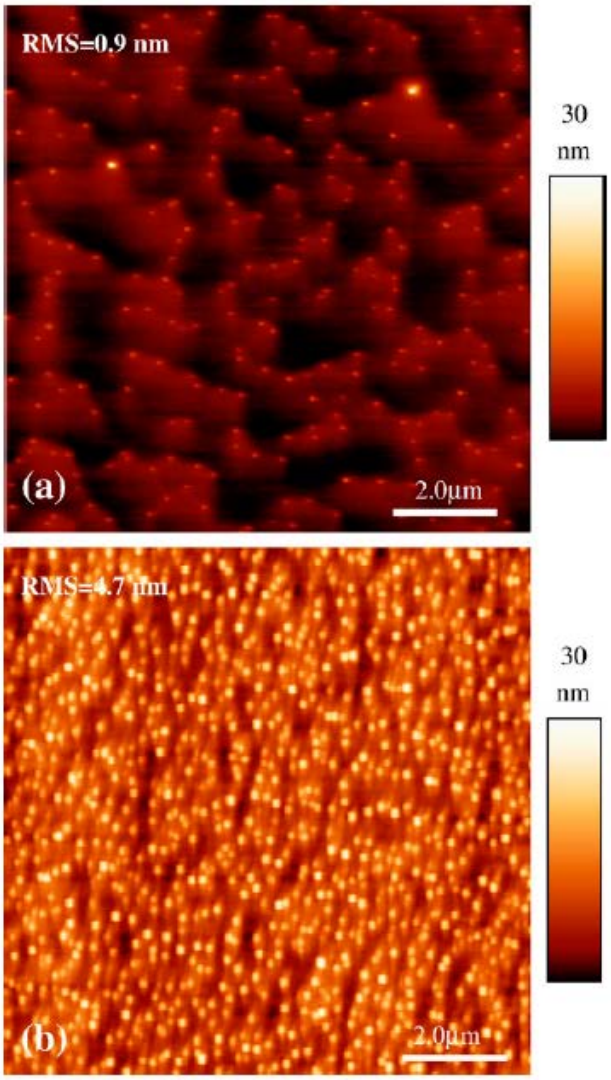

Fig. 1. AFM images of 5-nm-thick Co films deposited onto silicon surfaces at room temperature. (a) On Si(001) 2×1 surface: the average surface roughness (RMS) is 0.9 nm. (b) On Si(111) 7×7 surface: the RMS is 4.7 nm.

One of the major problems to obtain smooth and ferromagnetic films on Si substrates is the high reactivity between most transition metals with Si, which results in the formation of silicides. For metal deposition at high temperatures, various silicide phases can be formed and most silicides are not ferromagnetic (for example, $CoSi_2$ is metallic while $FeSi_2$ is semiconducting). Even for room temperature deposition, interface silicides can formed. For example, in the case of Co deposition on Si, it has been shown

by many groups [12–17] that for sub-monolayer of Co deposition, Co reacts with Si to form the $CoSi_2$ phase even at room temperature. When the Co coverage increases, the deposited film becomes less and less rich in Si and a pure Co layer can be formed after the deposition of about 4–5 ML.

Fig. 1 shows the surface morphology measured by AFM of 5-nm-thick Co film deposited on Si(001) and Si(111) surfaces at room temperature. For Co deposition on Si(001) substrate (Fig. 1a), the Co film consists of domains around 1–2 μm. The average surface roughness is 0.9 nm, which is three times higher than the thickness of an Al monolayer (1 ML of Al is ~0.284 nm). For Co deposition on Si(111) substrate (Fig. 1b), the surface consists of close-packed islands with a surface roughness as high as 4.7 nm. The high surface roughness observed for Co films deposited on Si at room temperature probably arises from a conjunction of two factors: low mobility of adatoms due to room temperature deposition and the formation of disordered silicide phases at the interface.

An approach, which may allow reducing the formation of disordered and undefined composition phase at the interface between transition metals and silicon is the use of a template layer at the interface. The idea is to organize the interface phase in order to form a well-defined compound instead of letting the system intermixing naturally. Bertoncini et al. [18,19] have used a thin disilicide MSi_2 layer (M=Co, Fe) prior to Fe deposition. This thin disilicide layer, prepared by deposition of some ML of Fe on Si at room temperature followed by annealing at ~550 °C, can act as a diffusion barrier of silicon substrate atom into the Fe overlayer. While it has been shown that high-quality

ferromagnetic films can be formed onto silicon substrate, no improvement in the surface roughness has been evidenced.

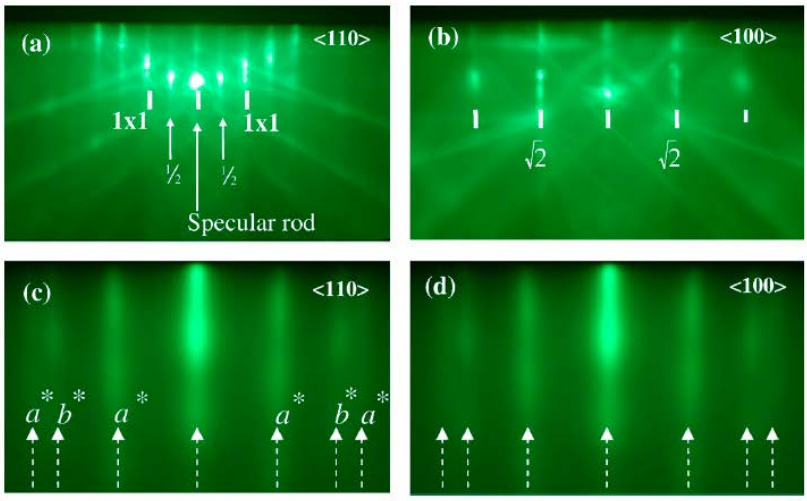

Fig. 2. RHEED patterns taken along <110> azimuth (patterns a and c) and <100> azimuth (patterns b and d). (a and b) Si(001)2 × 1 surface prior to growth. (c and d) 3-nm-thick Co film deposited on Si(001) at a substrate temperature of 300 °C.

Following this approach, we have deposited 2ML of Co on Si (001) substrate and undertaken thermal annealing up to 650 °C. This method is so-called solid-state epitaxy (SPE). Starting from a well-developed 2×1 surface, STM analyses indicated that the Si surface is completely covered by Co after deposition of 2ML and that the surface is highly disordered. We have annealed the sample at three temperatures: at 300 °C which corresponds to the formation of the Co_2Si phase, at 400 °C corresponding to CoSi and finally at 600–650 °C which corresponds to the formation of CoSi2 disilicide. Our analyses by STM reveal that the surface remains disordered after 10 min of annealing at 300 and up to 400 °C. Epitaxial structures, corresponding to $CoSi_2$ disilicide, are observed only after annealing at 600–650 °C. However, the $CoSi_2$ film is not continuous but rather composed of discrete islands or clusters and between these clusters STM images reveal the existence of clean silicon (observation of 2×1

reconstruction with A and B atomic steps). We have tried to deposit a 5-nmthick Co layer on these three surfaces: Co_2Si, CoSi and $CoSi_2$. Compared to Co films with the same thickness deposited directly on Si(001) shown in Fig. 1a, we did observe a slight improvement of the film surface morphology. However, by this way the average surface roughness still remains high. Detailed results of this work will be published later.

We have tried another method to grow the template layer by reactive deposition epitaxy (RDE), i.e. by deposition onto a hot substrate. Different growth temperatures have been experienced and, interestingly, at a substrate temperature of around 300 °C, i.e. temperature corresponding to the formation of the Co_2Si phase, an epitaxial and continuous film is formed. The results are depicted in Fig. 2. Fig. 2a and b show RHEED patterns taken along b110N and b100N azimuths of the clean Si(001) surface prior to Co deposition. 2×1 patterns are clearly observed, indicating that the surface is clean and smooth. The interdistance between <100> streaks is √2 times larger than that observed along the <110> azimuth, which is well correlated with the twofold symmetry of the Si (001) surface. The RHEED patterns taken along <110> and <100> azimuths during the deposition of a 2-nm-thick Co film at 300 °C are displayed in Fig. 2c and d. First of all, the observation of long streaks indicates that the Co_2Si film, formed by Co deposition at 300 °C, is smooth and epitaxial on silicon. This result is quite different to what observed for Co_2Si film prepared by Co deposition at room temperature followed by an anneal at 300 °C, of which no RHEED patterns were observed. A result of particular interest is that the RHEED patterns of Co_2Si film are independent of azimuth, the same pattern is indeed observed for all crystallographic directions. From Fig. 2c and d, we can identify two interdistances between streaks, which are the same in both

RHEED patterns and correspond to two in-plane vectors, a* and b* of the epitaxial film. This result suggests that the grown filmconsists of multidomains, each domain has its c-axis perpendicular to the film surface while the two in-plane axes, a and b, are randomly distributed. The formation of Co_2Si film in small domains can be explained by a large difference in crystal structures and lattice parameters between Si and Co_2Si. Silicon has a diamond structure with a lattice parameter of 0.543 nm while the Co_2Si structure is orthorhombic with lattice parameters a=0.711 nm, b=0.492 nm and c=0.374 nm. This may explain why at standard growth conditions, i.e. room temperature deposition followed by thermal annealing, it was not possible to form epitaxial Co_2Si films. X-ray diffraction analyses are now in progress in order to precisely determine the epitaxial relationships between Co_2Si and Si.

Once the Co_2Si template layer has been formed, the substrate temperature is reduced to room temperature for growing the bottom electrode (Co or CoFe). We provide, in Fig. 3, some characteristics of a 15-nm-thick Co layer overgrown on the template layer at room temperature. The film surface morphology measured by AFM is displayed in Fig. 3a. Compared to the Co film directly deposited on Si(001) (shown in Fig. 1a), one can state that the present film, having a thickness three times larger, but presents a surface roughness of ~2.4 times smaller.

Fig. 3b displays the evolution of Auger intensities of Co (51 eV) and Si (92 eV) peaks measured by means of Auger profilometry. The correlation of these two depth profiles and the intensity of Co peak, which remains fairly constant up to a depth of ~15 nm, indicate that the overgrown Co film is pure (i.e., ferromagnetic). A cross-sectional TEM image of the same sample is presented in Fig. 3c. The TEM image reveals that the

Co_2Si template layer is relatively uniform in thickness, the two interfaces it shares with Si substrate and with the Co overlayer are fairly abrupt. The Co overlayer is obviously polycrystalline since the deposition was done at room temperature but we can observe some texture in the film, which probably results from growth on an epitaxial template layer.

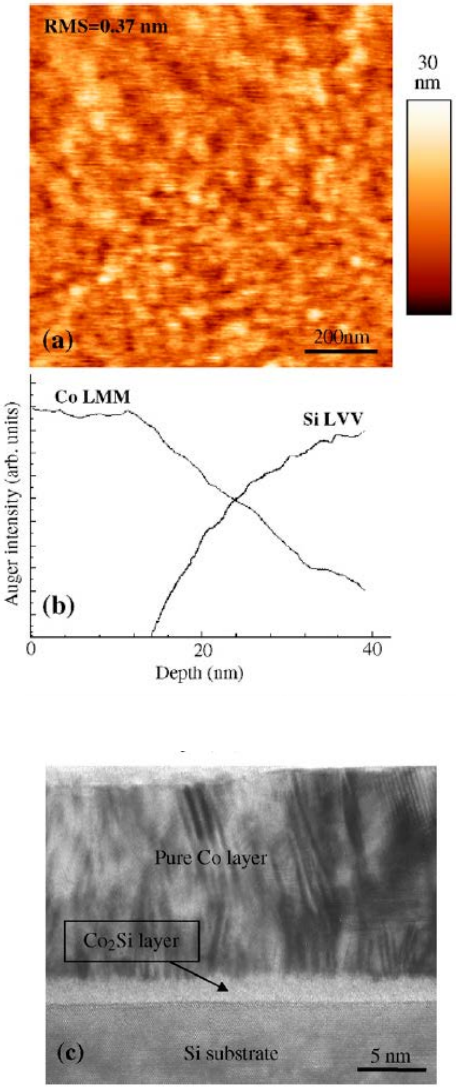

Fig. 3. Characteristics (morphology, composition and structure) of a 15-nm-thick Co film deposited at room temperature on the Co_2Si template layer. (a) AFM image revealing an average surface roughness of 0.37 nm. (b) HR-TEM indicating the formation of a pure Co layers on top of Co_2Si interfacial layer. (c) Depth profiles of Co and Si Auger intensities.

On such a relatively smooth Co surface, we have experienced layer-by-layer growth of the oxide barrier layer, which consists of successive cycles of Al deposition followed by oxidation using molecular oxygen. Both Al deposition and Al oxidation were carried out at room temperature. The Al thickness for each deposition is ~1 ML (0.284 nm). Two parameters, the oxygen pressure and the oxidation time, need to be controlled in order to determine the oxidation kinetics. Concerning the Al oxidation time, similar work, carried out in our group on the oxidation of 1ML of Al deposited on monocrystalline Ag surfaces, indicates that under an oxygen pressure of 2×10^{-6} Torr, the oxidation time, which is needed to completely oxidize 1ML of Al, is about 60 s [20]. Since the oxygen pressure used in the present work is much lower, we have therefore kept the oxidation time of 90 s in all experiments. It is worth noting that the oxidation kinetics of Al on Co electrode may be different compared to that of Al on noble metal surfaces but the above result on the Al/Ag system may give an order of magnitude on the oxidation time of a Al monolayer. Our purpose was to use a smallest oxidation time to reduce the oxidation of the buried Co electrode. However, we cannot rule out that either a fraction of Al monolayer is not oxidized or a fraction of buried Co monolayer is oxidized.

The dependence of Al oxidation on the oxygen pressure is shown in Fig. 4. The examined structures consist of 24 cycles of Al deposition/oxidation at two oxygen pressures of 1×10^{-8} and 5×10^{-7} Torr, which are covered with a 5-nm-thick Co layer (the total thickness of the oxide layer is ~8.86 nm). In Fig. 4a, corresponding to $PO_2=1\times10^{-8}$ Torr, the fact that the measured Al peak is located at 68 eVand the absence of oxygen signal in the depth profile clearly indicates that Al oxidation had not occurred.

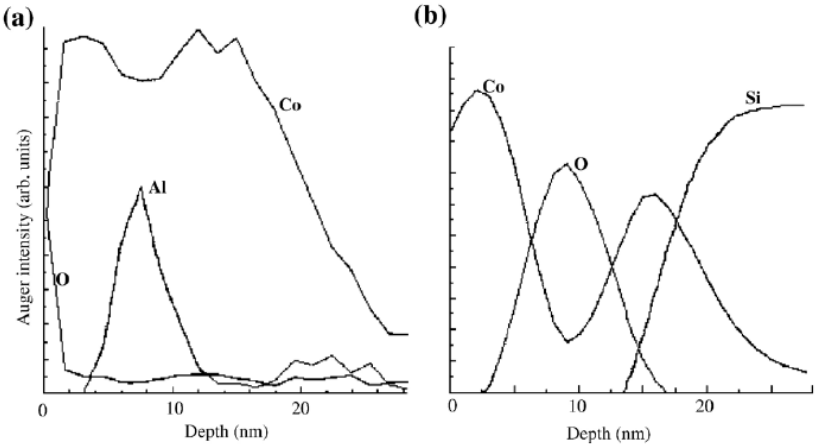

Fig. 4. Oxidation kinetics versus the pressure of oxygen flux obtained from Auger intensity depth profiles: (a) oxygen pressure of $\sim 1\times10^{-8}$ Torr; (b) oxygen pressure of $\sim 5\times10^{-7}$ Torr.

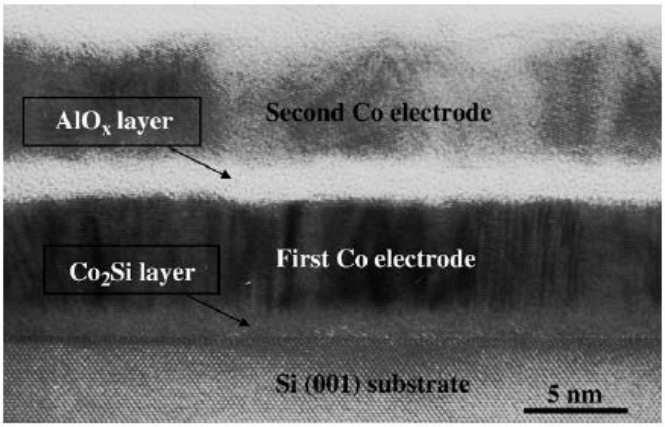

Fig. 5. Cross-sectional TEM image of a Co/AlO_x/Co junction grown on Si(001) substrate using Co_2Si as a template layer. The thickness of the oxide layer is ~1.5 nm. The oxide layer appears to be uniform in thickness and the interfaces with two ferromagnetic electrodes are relatively abrupt.

Note that the increase of the oxygen and the decrease of Co peaks at the surface region can be attributed to the film surface oxidation when exposing the sample in air. In Fig. 4b ($PO_2=5\times10^{-7}$ Torr), the presence of the oxygen peak (511 eV) and the decrease of the Co signal at the expected depth regions confirm that the Al layers have been oxidized. Note that in this case the Al peak is shifted to the low energy (55–57 eV).

However, due to the very close proximity of this peak with Co Auger peak (51 eV), this peak is not clearly resolved.

Displayed in Fig. 5 is a cross-sectional TEM image of a junction with structure of Co (5 nm)/AlO_x/Co (5 nm) grown on Si(001) substrate by using a template method. The oxide barrier layer was formed by 4 cycles Al deposition/oxidation at $PO_2=5\times10^{-7}$ Torr. Assuming that $d_{Al2O3}=1.3d_{Al}$, the expected thickness of the oxide layer is ~1.5 nm. This value is in good agreement that that measured from TEM image. A result of particular interest is that the thickness of the oxide layer is very uniform and the interfaces between the oxide layer and two Co electrodes are fairly abrupt.

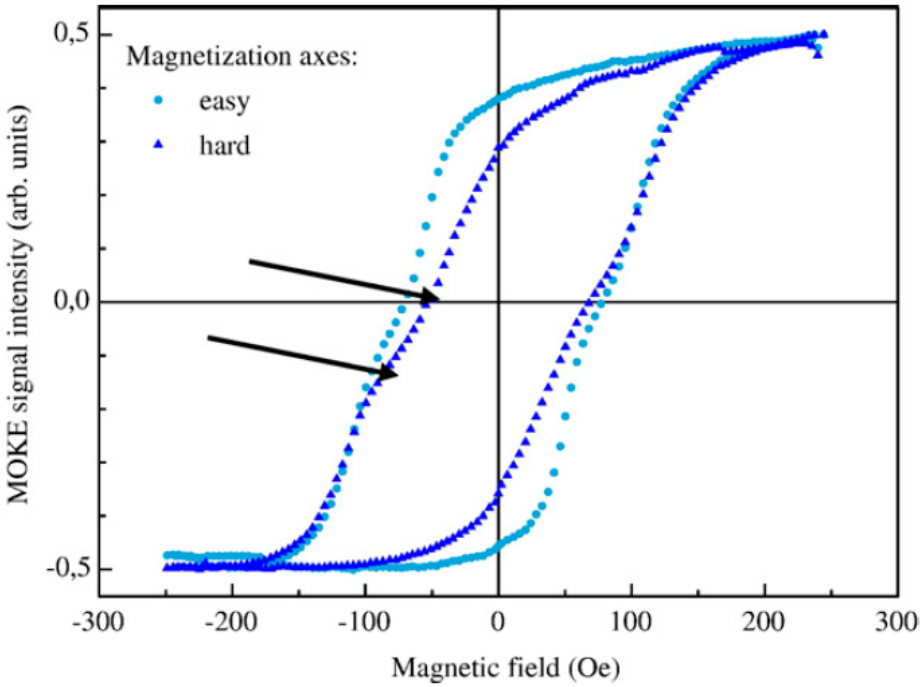

Fig. 6. MOKE hysteresis loops recorded at room temperature of a tunnel junction with structure Co (10 nm)/AlO_x (1.5 nm)/CoFe (15 nm). The field applied is along [110] direction (easy axis) and [−110] direction (hard axis).

In order to get information on the dielectric quality of the oxide barrier layer prepared by layer-by-layer method, we have realized tunnel junctions with structures of Co (10 nm)/AlO_x (1.5 nm)/CoFe (10 nm) and investigate the magnetic properties by means of MOKE. The measurements were carried out ex situ and at room temperature. Fig. 6 displays hysteresis loops of the above tunnel junctions with the field applied along two orthogonal directions [110] and [−110]. A slight magnetic anisotropy can be seen from the MOKE measurements, an easy axis loop is observed along [110] direction and a hard axis one observed along [−110] direction.Work is in process in order to determine the structure of the two ferromagnetic electrodes. From the above hysteresis loops, one can see a slight change of the magnetization (indicated by arrows) from the bottom electrode to the top one. While the detailed stoichiometry of the oxide layer remains to be determined, the above result indicates the very thin oxide layer, prepared by layer-by-layer method, can act as a tunnel barrier in magnetic tunnel junctions.

Conclusion

In summary, we have presented a new approach to grow ferromagnetic films and magnetic tunnel junctions onto silicon substrates by using Co_2Si as a template layer. This template layer, prepared by Co deposition on Si at a temperature of ~300 °C, is epitaxial and fairly smooth. We have also demonstrated the feasibility of the layer-by-layer method to grow nanometer-scaled oxide AlO_x layer. While much still remains to be done in order to determine the quality of the oxide layer, we have shown that such an oxide layer can act as a tunnel barrier in magnetic tunnel junctions. It is important to emphasize that oxide layer prepared by such a method is very uniform in thickness and has fairly abrupt interfaces with ferromagnetic electrodes. We note that if further work

indicates that such an oxide is not stoichiometric alumina (Al_2O_3), other oxidant species like ozone and atomic oxygen can be used to increase the chemical reactivity.

References

[1] J.S. Moodera, G. Mathon, J. Magn. Magn. Mater. 200 (1999) 248.

[2] S.S. Parkin, K.P. Roche, M.G. Samant, P.M. Rice, R.B. Beyers, J. Appl. Phys. 85 (1999) 5828.

[3] G. Prinz, Science 282 (1998) 1660.

[4] M. Jullière, Phys. Lett. 54 (1975) 225.

[5] Chando Park, Jian-Gang Zhu, Matthew T. Moneck, Yingguo Peng, David E. Laughlin, J. Appl. Phys. 99 (2006) 08A901.

[6] S. Ikeda, J. Hayakawa, Y.M. Lee, R. Sasaki, T. Meguro, F. Matsukura, H. Ohno, Jpn. J. Appl. Phys. 44 (2005) L1442.

[7] D.D. Djayaprawira, Koji Tsunekawa, Motonobu Nagai, Hiroki Maehara, Shinji Yamagata, Naoki Watanabe, Appl. Phys. Lett. 86 (2005) 092502.

[8] R.C. Sousa, J.J. Sun,V. Soares, P.P. Freitas,Appl. Phys. Lett. 73 (1998) 3288.

[9] K. Sin, M. Mao, C. Chien, L. Miloslavsky, S. Funada, H. Tong, S. Grupta, IEEE Trans. Magn. 36 (2000) 2818.

[10] Y. Ando, M. Hayashi, S. Iura, K. Yaoita, C.C. Yu, H. Kubota, T. Miyazaki, J. Phys., D, Appl. Phys. 35 (2002) 2415.

[11] A. Ishizaka, Y. Shiraki, J. Electrochem. Soc. 133 (1986) 666.

[12] F. Boscherini, J.J. Joyce, M.W. Ruckman, J.H. Weaver, Phys. Rev., B 35 (1887) 4216.

[13] G. Rangelov, P. Augustin, J. Stober, T. Frauster, Surf. Sci. 307 (1994) 264.

[14] J. Derrien, Surf. Sci. 168 (1986) 171.

[15] C. Pirri, J.C. Peruchetti,G.Gewinner, J.Derrien, Phys.Rev.,B29 (1984) 3391.

[16] R. Stader, C. Schwarz,H. Sirringhaus,H. vonKänel, Surf. Sci. 271 (1992) 355.

[17] J.S. Pan, R.S. Liu, Z. Zhang, S.W. Poon,W.J. Ong, E.S. Tok, Surf. Sci. 600 (2006) 1308.

[18] P. Bertoncini, D. Berling, P. Wetzel, A. Mehdaoui, B. Loegel, G. Gewinner, C. Ulhaq-Bouillet, V. Pierron-Bohnes, Surf. Sci. 454–456 (2000) 755.

[19] P.Wetzel, P. Bertoncini, D. Berling, A.Mehdaoui, B. Loegel, D. Bolmont, G. Gewinner, C. Ulhaq-Bouillet, V. Pierron-Bohnes, Surf. Sci. 499 (2002) 210.

[20] H. Oughaddou, S.Vizzini, B. Aufray, B. Ealet, J.P. Bibérian, L. Ravel, J.-M. Gay, F.A. d'Avitaya, J. Phys. IV Fr. 132 (2006) 269.